

## Higgs Boson Production in High Energy Lepton-Nucleon Scattering

Zenrō HIOKI<sup>\*)</sup>, Shoichi MIDORIKAWA and Hiroyuki NISHIURA<sup>\*\*)†)</sup>

*Research Institute for Fundamental Physics,  
Kyoto University, Kyoto 606*

*\*Department of Physics, Kyoto University, Kyoto 606*

(Received January 6, 1983)

Higgs boson productions are studied in high energy  $\nu(\bar{\nu})N$  and  $l^{\pm}N$  scatterings. Total cross-sections are calculated at the lowest order of perturbation by taking into account two kinds of mechanisms, i. e., bremsstrahlungs from (I) strange- and charm-quark and from (II)  $W^{\pm}$ ,  $Z$  boson, and detailed numerical results are presented in the framework of QCD improved parton model. In  $\nu N$  process, it is shown that the contribution of the mechanism (II) is dominant for an extensive range of the energy although that of the mechanism (I) increases rapidly with energy. On the contrary, both mechanisms give comparable contributions in  $l^{\pm}N$  processes. The total cross-sections are found to be rather small for both reactions even at very high energy.

### § 1. Introduction

It is widely accepted that we have a correct theory of the electroweak interactions, namely the standard  $SU(2) \times U(1)$  gauge theory.<sup>1)</sup> All phenomena of the weak interaction described in the (current)  $\times$  (current) form are consistently fitted by using the only one parameter called Weinberg angle  $\sin^2 \theta_w \approx 0.23 \pm 0.02$ . As a next step for the test of the theory, much effort should be and will be directed towards possible detection of  $W^{\pm}$ ,  $Z$  and higher order effects.<sup>2)</sup>

Unfortunately, however, none of the above arguments can be regarded as the studies of "spontaneously broken" gauge theory. In relation to this point it is crucial to search for the Higgs particle ( $H$ ). Though the standard theory may be correct only as an effective theory at the low energy region and the Higgs boson may be composite, we believe that it is important to make effort for assessing the feasibility to detect  $H$  within the standard scheme. The Higgs particle is notoriously elusive, and much is not yet known on its property. Theoretical considerations suggest its mass value to lie somewhere between 5 GeV<sup>3)</sup> and 1 TeV.<sup>4)</sup>

There are some crude estimates of the Higgs boson production rate in lepton-

<sup>\*)</sup> Fellow of the Osaka Univ. Yukawa Foundation.

<sup>\*\*)†)</sup> Fellow of the Japan Society for the Promotion of Science.

<sup>†)</sup> Present address: Institute of Physics, College of General Education, Osaka University, Toyonaka

nucleon scattering,<sup>5)</sup> assuming the Higgs boson to be emitted dominantly from an internal line of a weak boson. In a previous paper Yoshimura and one of the authors (S. M.)<sup>6)</sup> stressed the large rate of the Higgs boson production off heavy quarks in  $ep$  scattering, and gave a rough estimate based on the approximation of soft emission. Abad et al. also reached the same conclusion by considering the  $\gamma g \rightarrow q\bar{q}H$  subprocess.<sup>7)</sup>

The aim of the present paper is to improve the existing calculations by taking exact account of both the bremsstrahlung from (I) strange- and charm-quark and from (II)  $W^\pm, Z$  boson. In the mechanism (I), the production rate depends on the still unknown contents of charm-quark (generally, heavy quark) states in the nucleon. Recently the possibility of large intrinsic charm-quark states has been discussed in the literature,<sup>8)</sup> which makes our investigation more important.

This paper is organized as follows. In § 2 we give the cross-section for the process,  $\nu_l(\bar{\nu}_l)+N \rightarrow l^-(l^+)+H+X$ , and  $l^\pm+N \rightarrow l^\pm+H+X$ , by using a quark-parton model. In § 3 the results of numerical computations are given with the QCD improved parton distribution function à la Buras and Gaemers.<sup>9)</sup> Calculations are also made for the case of large intrinsic charm distribution. Section 4 is devoted to summary and discussions.

§ 2. Calculations of the cross-sections

In this section, we calculate the total cross-sections  $\sigma(\nu_l(\bar{\nu}_l)N \rightarrow l^-(l^+)HX)$  and  $\sigma(l^\pm N \rightarrow l^\pm HX)$  ( $l=e, \mu$ ). At first, the cross-sections for the elementary processes,  $\nu_l(\bar{\nu}_l)+q \rightarrow l^-(l^+)+H+q'$  and  $l^\pm+q \rightarrow l^\pm+H+q$  are evaluated at the lowest order of perturbation. Then, integrating the products of these cross-sections and the parton distribution functions, we obtain the physical cross-

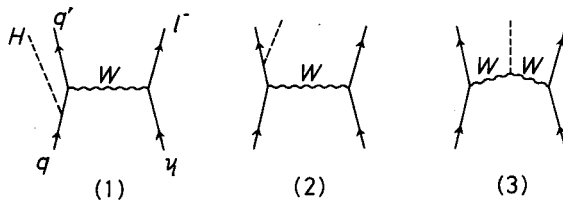
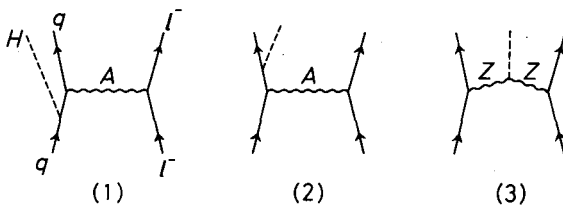


Fig. 2(a) The relevant Feynman diagrams for  $\nu_l q \rightarrow l^- H q'$  process.



(b) The relevant Feynman diagrams for  $l^- q \rightarrow l^- H q$  process ( $l=e$  or  $\mu$ ). ( $A$  means the photon propagator.)

sections.

The relevant Feynman diagrams under the approximation  $m_\nu = m_l = 0$  are shown in Fig. 2(a) for  $\nu q$  process and in Fig. 2(b) for  $l^- q$  process. In the following, we further make the approximation  $m_u = m_d = 0$  and  $\sin\theta_c$  (Cabibbo angle) = 0. Therefore, only the diagram (3) in Figs 2(a) and 2(b) needs to be taken into account when the initial quark is  $u(\bar{u})$  or  $d(\bar{d})$ . In the following we call the production mechanism of the diagrams (1) and (2) "mechanism I" and that of the diagram (3) "mechanism II".

The matrix elements are expressed as follows :

$\nu q \rightarrow l^- H q'$  process

$$M_1^\nu = G_1^\nu \bar{u}_l(k') \gamma_\alpha (1 - \gamma_5) u_\nu(k) \cdot \bar{u}_{q'}(p') (m_f + \not{p}' + \not{p}_H) \gamma^\alpha (1 - \gamma_5) u_q(p), \quad (2.1a)$$

$$M_2^\nu = G_2^\nu \bar{u}_l(k') \gamma_\alpha (1 - \gamma_5) u_\nu(k) \cdot \bar{u}_{q'}(p') \gamma^\alpha (1 - \gamma_5) (m_i + \not{p} - \not{p}_H) u_q(p), \quad (2.1b)$$

$$M_3^\nu = G_3^\nu \bar{u}_l(k') \gamma_\alpha (1 - \gamma_5) u_\nu(k) \cdot \bar{u}_{q'}(p') \gamma^\alpha (1 - \gamma_5) u_q(p), \quad (2.1c)$$

$$G_1^\nu \equiv \frac{g^3 m_f}{16 M_W} \frac{1}{q^2 - M_W^2} \frac{1}{m_f^2 - (\not{p}' + \not{p}_H)^2}, \quad (2.1d)$$

$$G_2^\nu \equiv \frac{g^3 m_i}{16 M_W} \frac{1}{q^2 - M_W^2} \frac{1}{m_i^2 - (\not{p} - \not{p}_H)^2}, \quad (2.1e)$$

$$G_3^\nu \equiv \frac{g^3 M_W}{8} \frac{1}{q^2 - M_W^2} \frac{1}{(q - \not{p}_H)^2 - M_W^2}, \quad (2.1f)$$

$$(q^2 \equiv (k - k')^2)$$

where  $g$  is the  $SU(2)$  coupling constant,  $p_H$  is the momentum of the Higgs boson,  $m_i(m_f)$  and  $M_W$  denote the masses of initial (final) quark and  $W^\pm$  boson respectively.

$l^- q \rightarrow l^- H q'$  process

$$M_1^l = G_1^l \bar{u}_l(k') \gamma_\alpha u_l(k) \cdot \bar{u}_{q'}(p') (m_q + \not{p}' + \not{p}_H) \gamma^\alpha u_q(p), \quad (2.2a)$$

$$M_2^l = G_2^l \bar{u}_l(k') \gamma_\alpha u_l(k) \cdot \bar{u}_{q'}(p') \gamma^\alpha (m_q + \not{p} - \not{p}_H) u_q(p), \quad (2.2b)$$

$$M_3^l = G_3^l \bar{u}_l(k') \gamma_\alpha (V_l - \gamma_5) u_l(k) \cdot \bar{u}_{q'}(p') \gamma^\alpha (V_q - \gamma_5) u_q(p), \quad (2.2c)$$

$$G_1^l \equiv e^2 Q_q \frac{gm_q}{2M_W} \frac{1}{q^2} \frac{1}{m_q^2 - (p' + p_H)^2}, \quad (2.2d)$$

$$G_2^l \equiv e^2 Q_q \frac{gm_q}{2M_W} \frac{1}{q^2} \frac{1}{m_q^2 - (p - p_H)^2}, \quad (2.2e)$$

$$G_3^l \equiv \frac{-g^3 M_Z}{16 \cos^3 \theta_w} \frac{|Q_q|}{Q_q} \frac{1}{q^2 - M_Z^2} \frac{1}{(q - p_H)^2 - M_Z^2}, \quad (2.2f)$$

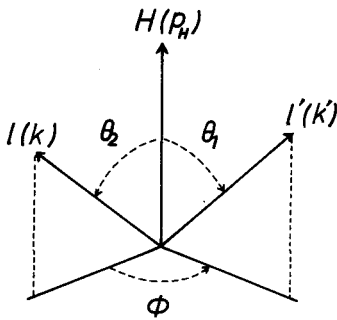


Fig. 2(c) CM-frame axes and angles used in this paper.  $l$  and  $l'$  denote the initial and final leptons respectively ( $l = \nu, e, \mu$  and  $l' = e, \mu$ ). The letters in the parentheses express the corresponding momentum. The initial and final quarks are not shown.

where  $Q_q$  and  $m_q$  are the electric charge (in  $|e|$  unit) and the mass of the quark,  $M_Z$  denotes  $Z$  boson mass, and

$$V_l = 1 - 4 \sin^2 \theta_w, \quad (2.3a)$$

$$V_q = \begin{cases} 1 - \frac{8}{3} \sin^2 \theta_w & \text{for } Q_q = \frac{2}{3}, \\ 1 - \frac{4}{3} \sin^2 \theta_w & \text{for } Q_q = -\frac{1}{3}. \end{cases} \quad (2.3b)$$

After some tedious but straightforward calculations we find the cross-sections in the lepton-quark CM frame (shown in Fig. 2(c)) as

$$\begin{aligned} & \frac{d^4 \sigma}{dE_l' d \cos \theta_1 d \cos \theta_2 d \phi} (\nu q \rightarrow l^- H q') \\ &= \frac{1}{16(2\pi)^4 (\hat{s} - m_q^2)} \frac{|\mathbf{p}_H|^2 E_l'}{E_l' E_H \cos \theta_1 + |\mathbf{p}_H| (\sqrt{\hat{s}} - E_l')} \frac{1}{2} \sum_{\text{spin}} |M_1^\nu + M_2^\nu + M_3^\nu|^2, \\ & (\hat{s} \equiv (p + k)^2, k' = (E_l', \mathbf{k}'), p_H = (E_H, \mathbf{p}_H)) \end{aligned} \quad (2.4)$$

$$\sum_{\text{spin}} |M_1^\nu|^2 = 256 (G_1^\nu)^2 (pk) [2\{2m_f^2 + (p' p_H)\}(p_H k') + (4m_f^2 - m_H^2)(p' k')], \quad (2.4a)$$

$$\sum_{\text{spin}} |M_2^\nu|^2 = 256 (G_2^\nu)^2 (p' k') [-2\{2m_i^2 - (p p_H)\}(p_H k) + (4m_i^2 - m_H^2)(pk)], \quad (2.4b)$$

$$\sum_{\text{spin}} |M_3^\nu|^2 = 256 (G_3^\nu)^2 (pk)(p' k'), \quad (2.4c)$$

$$\begin{aligned} \sum_{\text{spin}} \text{Re}(M_1^\nu M_2^{\nu*}) \\ = 256 G_1^\nu G_2^\nu m_i m_f \{2(pk) - (p_H k)\} \{2(p'k') + (p_H k')\}, \end{aligned} \quad (2.4d)$$

$$\sum_{\text{spin}} \text{Re}(M_1^\nu M_3^{\nu*}) = 256 G_1^\nu G_3^\nu m_f (pk) \{2(p'k') + (p_H k')\}, \quad (2.4e)$$

$$\sum_{\text{spin}} \text{Re}(M_2^\nu M_3^{\nu*}) = 256 G_2^\nu G_3^\nu m_i (p'k') \{2(pk) - (p_H k)\}, \quad (2.4f)$$

and

$$\begin{aligned} \frac{d^4\sigma}{dE_l' d \cos\theta_1 d \cos\theta_2 d\phi} (l^- q \rightarrow l^- H q) \\ = \frac{1}{16(2\pi)^4 (\hat{s} - m_q^2)} \frac{|\mathbf{p}_H|^2 E_l'}{E_l' E_H \cos\theta_1 + |\mathbf{p}_H|(\sqrt{\hat{s}} - E_l')} \frac{1}{4} \sum_{\text{spin}} |M_1^l + M_2^l + M_3^l|^2, \end{aligned} \quad (2.5)$$

$$\begin{aligned} \sum_{\text{spin}} |M_1^l|^2 &= 32 (G_1^l)^2 [2\{(p'p_H) + 2m_q^2\} \{(pk)(p_H k') + (pk')(p_H k)\} \\ &\quad + (4m_q^2 - m_H^2) \{(pk)(p'k') + (pk')(p'k)\} \\ &\quad - m_q^2 \{4(p'p_H) + 4m_q^2 + m_H^2\} (kk')], \end{aligned} \quad (2.5a)$$

$$\begin{aligned} \sum_{\text{spin}} |M_2^l|^2 &= 32 (G_2^l)^2 [2\{(pp_H) - 2m_q^2\} \{(p'k)(p_H k') + (p'k')(p_H k)\} \\ &\quad + (4m_q^2 - m_H^2) \{(pk)(p'k') + (pk')(p'k)\} \\ &\quad + m_q^2 \{4(pp_H) - 4m_q^2 - m_H^2\} (kk')], \end{aligned} \quad (2.5b)$$

$$\begin{aligned} \sum_{\text{spin}} |M_3^l|^2 &= 32 (G_3^l)^2 [(V_l^2 + 1)(V_q^2 + 1) \{(pk)(p'k') + (pk')(p'k)\} \\ &\quad - m_q^2 (V_l^2 + 1)(V_q^2 - 1)(kk') + 4V_l V_q \{(pk)(p'k') - (pk')(p'k)\}], \end{aligned} \quad (2.5c)$$

$$\begin{aligned} \sum_{\text{spin}} \text{Re}(M_1^l M_2^{l*}) &= 32 G_1^l G_2^l [2m_q^2 \{2(pk)(p'k') + 2(pk')(p'k) - (p_H k)(p_H k') \\ &\quad - (p_H k)(p'k') + (p_H k)(pk') - (p_H k')(p'k) \\ &\quad + (p_H k')(pk) + (pp_H)(kk') - (p'p_H)(kk')\} \\ &\quad - m_H^2 \{(pk)(p'k') + (pk')(p'k) - (pp')(kk')\} \end{aligned}$$

$$\begin{aligned}
 & + (p' p_H) \{ (pk)(p_H k') + (pk')(p_H k) \} \\
 & + (p p_H) \{ (p' k)(p_H k') + (p' k')(p_H k) \} \\
 & - 2(p p') (p_H k)(p_H k') - 4m_q^4 (kk'), \tag{2.5d}
 \end{aligned}$$

$$\begin{aligned}
 \sum_{\text{spin}} \text{Re}(M_1' M_3'^*) &= 32m_q G_1' G_3' [2(V_l V_q + 1)(pk)(p' k') + 2(V_l V_q - 1)(pk')(p' k) \\
 & + (V_l V_q - 1)(pk')(p_H k) + (V_l V_q + 1)(pk)(p_H k') \\
 & - V_l V_q \{ 2m_q^2 + (p' p_H) \} (kk') - (p_H k)(p' k') + (p_H k')(p' k)], \tag{2.5e}
 \end{aligned}$$

$$\begin{aligned}
 \sum_{\text{spin}} \text{Re}(M_2' M_3'^*) &= 32m_q G_2' G_3' [2(V_l V_q + 1)(pk)(p' k') + 2(V_l V_q - 1)(pk')(p' k) \\
 & - (V_l V_q - 1)(p_H k')(p' k) - (V_l V_q + 1)(p_H k)(p' k') \\
 & - V_l V_q \{ 2m_q^2 - (p p_H) \} (kk') + (pk)(p_H k') - (pk')(p_H k)]. \tag{2.5f}
 \end{aligned}$$

The cross-sections of  $\bar{\nu}q$  and  $l^+q$  processes can be obtained by the replacement  $k \rightarrow -k'$  and  $k' \rightarrow -k$  in Eqs. (2.4a)~(2.4f) and (2.5a)~(2.5f). ( $\sigma(\nu\bar{q})$ ,  $\sigma(\nu\bar{q})$ ,  $\sigma(l^+\bar{q})$  and  $\sigma(l^-\bar{q})$  are equal to  $\sigma(\nu q)$ ,  $\sigma(\bar{\nu}q)$ ,  $\sigma(l^-q)$  and  $\sigma(l^+q)$  respectively.)

The total cross-sections of the lepton-nucleon processes are calculated by using the quark-parton model,

$$\begin{aligned}
 & \sigma\left(\begin{matrix} \nu \\ l^- \end{matrix} N \rightarrow l^- H X\right) \\
 &= \sum_q \int dx dE_i' d \cos \theta_1 d \cos \theta_2 d\phi q(x, Q^2) \\
 & \times \frac{d^4 \sigma}{dE_i' d \cos \theta_1 d \cos \theta_2 d\phi} \left( \begin{matrix} \nu \\ l^- \end{matrix} q \rightarrow l^- H \begin{pmatrix} q' \\ q \end{pmatrix} \right). \\
 & (q(x, Q^2): \text{parton distribution function, } Q^2 \equiv -(k-k')^2) \tag{2.6)*}
 \end{aligned}$$

In the actual calculations, we assume that  $\hat{s} = xs + m_i^2$  ( $s \equiv (k+P)^2$ ,  $P$ : nucleon

\*) Here appears an ambiguity: Should we use  $Q^2 = -(k-k')^2$  or  $Q^2 = -(p-p')^2 = -(k-k'-p_H)^2$  in  $q(x, Q^2)$ ? It is considered natural to use  $Q^2 = -(k-k')^2$  ( $Q^2 = -(p-p')^2$ ) for diagrams (1) and (2) (for diagram (3)). We make a choice of  $Q^2 = -(k-k')^2$  here. (We have confirmed that another choice makes only small difference.)

momentum) and that the momenta of quarks in the initial and final states are all on the mass-shell. The range of integration is fixed by the common area determined by

$$\begin{aligned} \frac{\hat{s} - (m_f + m_H)^2}{2\sqrt{\hat{s}}} &\geq E_i' \geq 0, \\ \pi &\geq \theta_1, \quad \theta_2 \geq 0, \\ 2\pi &\geq \phi \geq 0, \\ |\mathbf{p}_H| &\geq 0, \end{aligned} \tag{2.7}$$

where

$$\begin{aligned} |\mathbf{p}_H| = & \frac{1}{2\{(\sqrt{\hat{s}} - E_i')^2 - E_i'^2 \cos^2 \theta_1\}} \left[ -E_i' \cos \theta_1 (\hat{s} - 2E_i' \sqrt{\hat{s}} + m_H^2 - m_f^2) \right. \\ & \left. + (\sqrt{\hat{s}} - E_i') \sqrt{(\hat{s} - 2E_i' \sqrt{\hat{s}} + m_H^2 - m_f^2)^2 - 4m_H^2 \{(\sqrt{\hat{s}} - E_i')^2 - E_i'^2 \cos^2 \theta_1\}} \right]. \end{aligned} \tag{2.8}$$

The numerical computations are performed in the next section.

### § 3. Numerical results

We here derive numerical results in detail. As the parton distribution function, we use the QCD improved one,  $q(x, Q^2)$  ( $q(x, Q_0^2)$  for the region  $Q^2 < Q_0^2 = 1.8 \text{ GeV}^2$ ), formulated by Buras and Gaemers (with  $\Lambda_{\text{QCD}} = 0.3 \text{ GeV}$ )<sup>9)</sup> and also the one without QCD effects,  $q(x) = q(x, Q_0^2)$ . The integrations in Eq. (2.6) are performed by Monte Carlo method<sup>10)</sup> and the results are given in Tables III(a) and (b) for the two representative values of Higgs mass,  $m_H = 10$  and  $50 \text{ GeV}$ . As for the other parameters we have taken  $m_\nu = m_l = m_u = m_d = 0$ ,  $m_s = 0.3 \text{ GeV}$  and  $m_c = 1.5 \text{ GeV}$ , and  $M_W = 77.7 \text{ GeV}$  and  $M_Z = 88.6 \text{ GeV}$  which correspond to  $\sin^2 \theta_w = 0.23$ .

Concerning the charm-quark distribution function in the nucleon, we have used (i) the one in Ref. 9) (hereafter we call it the "ordinary" charm distribution) and also (ii) rather large (1%) distribution which is motivated from the recent discussion by Brodsky et al.<sup>8)</sup> (hereafter "large" charm distribution). In the latter case we have assumed the distribution functions

$$c(x, Q^2) = \bar{c}(x, Q^2) = 0.55s(x, Q^2), \tag{3.1}$$

( $s(x, Q^2)$ ): strange-quark distribution function)

which correspond to the momentum fraction of charm-quark of 1% at  $Q^2=1.8$  GeV<sup>2</sup>. Strictly speaking, this assumption does not reflect the assertion in Ref.8) that charm-quarks are “rare but not wee”, i. e., the  $x$ -distribution is different from that given in Ref. 8). However, we have assumed this simple form here since we are only interested in the total cross-sections in the present paper.

For the  $\nu(\bar{\nu})N$  process, the dependences of the total cross-section on the initial Laboratory energy  $E_{\nu(\bar{\nu})}$  are shown in Fig. 3(a). The comparison of the contribution of the Higgs boson production from the strange- and charm-quarks (mechanism I) with the one from the virtual weak gauge boson  $W^\pm$  (mechanism II) are made in Fig. 3(b). We have shown there the ratio of the total cross-section due to the mechanism I only ( $\sigma_{(1)+(2)}$ ) to the one due to both the mechanisms I and II ( $\sigma_{(1)+(2)+(3)}$ ). The productions from heavy quarks are found to

Table III(a) The total cross-sections of the Higgs boson production for  $\nu_l N \rightarrow l^- H X$  and  $\bar{\nu}_l N \rightarrow l^+ H X$  processes. The cross-sections are given in unit of  $10^{-39}$  cm<sup>2</sup> for  $m_H=10$  and 50 GeV by using (1) QCD-improved parton model with ordinary charm distribution function by Buras and Gaemers, and (2) naive parton model, i.e., without QCD effects.  $m_H$  is the Higgs boson mass and  $E_{\nu(\bar{\nu})}$  is the Lab-energy of  $\nu_l(\bar{\nu}_l)$ .

[10 <sup>-39</sup> cm <sup>2</sup> unit]				
$\sigma(\nu_l N \rightarrow l^- H X)$				
$E_\nu(\text{GeV})$	$m_H=10$ GeV		$m_H=50$ GeV	
	(1)	(2)	(1)	(2)
10 <sup>2</sup>	1.5 × 10 <sup>-7</sup>	2.8 × 10 <sup>-7</sup>	—	—
5 × 10 <sup>2</sup>	3.2 × 10 <sup>-3</sup>	6.6 × 10 <sup>-3</sup>	—	—
10 <sup>3</sup>	3.1 × 10 <sup>-2</sup>	6.4 × 10 <sup>-2</sup>	—	—
5 × 10 <sup>3</sup>	1.4	2.7	9.5 × 10 <sup>-3</sup>	3.1 × 10 <sup>-2</sup>
10 <sup>4</sup>	4.7	8.7	2.1 × 10 <sup>-1</sup>	5.8 × 10 <sup>-1</sup>
5 × 10 <sup>4</sup>	4.3 × 10	6.2 × 10	1.1 × 10	2.1 × 10

$\sigma(\bar{\nu}_l N \rightarrow l^+ H X)$				
$E_{\bar{\nu}}(\text{GeV})$	$m_H=10$ GeV		$m_H=50$ GeV	
	(1)	(2)	(1)	(2)
10 <sup>2</sup>	8.5 × 10 <sup>-8</sup>	1.4 × 10 <sup>-7</sup>	—	—
5 × 10 <sup>2</sup>	1.6 × 10 <sup>-3</sup>	2.9 × 10 <sup>-3</sup>	—	—
10 <sup>3</sup>	1.5 × 10 <sup>-2</sup>	2.9 × 10 <sup>-2</sup>	—	—
5 × 10 <sup>3</sup>	7.6 × 10 <sup>-1</sup>	1.4	5.7 × 10 <sup>-3</sup>	1.7 × 10 <sup>-2</sup>
10 <sup>4</sup>	2.9	5.2	1.4 × 10 <sup>-1</sup>	3.8 × 10 <sup>-1</sup>
5 × 10 <sup>4</sup>	3.5 × 10	5.1 × 10	9.1	1.8 × 10



increase rapidly, which shows the enhancement of the sea component characteristic of QCD effects. The difference between the solid line (ordinary charm distribution case) and the dashed line (large charm distribution case) becomes smaller and smaller as the energy increases, which shows that  $SU(4)$  symmetry of parton sea components begins to be restored at very high energy. However, it is also found that the contribution of the mechanism II is dominant over the extensive range of the energy.

The incident energy dependences of the total cross-sections  $\sigma(l^\pm N \rightarrow l^\pm HX)$  are shown in Fig. 3(c) both for the cases of the ordinary and large charm-quark distributions. In the case of the large charm distribution (dashed line), the total cross-section for  $m_H=10$  GeV is enhanced in comparison with the ordinary case (solid line). This enhancement shows the fact that the mechanisms I and II are both important for  $l^\pm N \rightarrow l^\pm HX$  processes in contrast to the  $\nu N$  case as pointed out in Ref. 6). In this  $l^- N$  case, the restoration of  $SU(4)$  symmetry in the parton sea component does not proceed rapidly in comparison with the  $\nu N$  case, i. e., the sizable difference between the solid and dashed lines remains even at  $E_l \geq 10^4$  GeV. This comes from the low  $Q^2$  dominance in the mechanism I due to the photon propagator. Similar tendencies are also found for the  $l^+ N$  processes as

Table III(b) The total cross-sections of the Higgs boson production for  $l^- N \rightarrow l^- HX$  and  $l^+ N \rightarrow l^+ HX$  processes. The cross-sections are given in unit of  $10^{-39}$  cm<sup>2</sup> for  $m_H=10$  and 50 GeV in the cases of (1), (2) in Table III(a) and (3) QCD-improved parton model with the large charm distribution in the text.

[10<sup>-39</sup> cm<sup>2</sup> unit]

$\sigma(l^- N \rightarrow l^- HX)$

$E_l(\text{GeV})$	$m_H=10$ GeV			$m_H=50$ GeV		
	(1)	(2)	(3)	(1)	(2)	(3)
$10^2$	$4.7 \times 10^{-8}$	$6.3 \times 10^{-8}$	$6.7 \times 10^{-8}$	—	—	—
$5 \times 10^2$	$1.4 \times 10^{-3}$	$9.2 \times 10^{-4}$	$8.3 \times 10^{-3}$	—	—	—
$10^3$	$7.7 \times 10^{-3}$	$5.5 \times 10^{-3}$	$5.1 \times 10^{-2}$	—	—	—
$5 \times 10^3$	$1.7 \times 10^{-1}$	$2.1 \times 10^{-1}$	$5.2 \times 10^{-1}$	$7.1 \times 10^{-4}$	$2.3 \times 10^{-3}$	$7.3 \times 10^{-4}$
$10^4$	$5.2 \times 10^{-1}$	$7.0 \times 10^{-1}$	$9.7 \times 10^{-1}$	$1.8 \times 10^{-2}$	$4.9 \times 10^{-2}$	$1.8 \times 10^{-2}$
$5 \times 10^4$	4.5	6.3	4.9	1.1	2.2	1.1

$\sigma(l^+ N \rightarrow l^+ HX)$

$E_l(\text{GeV})$	$m_H=10$ GeV			$m_H=50$ GeV		
	(1)	(2)	(3)	(1)	(2)	(3)
$10^2$	$4.7 \times 10^{-8}$	$4.9 \times 10^{-8}$	$6.2 \times 10^{-8}$	—	—	—
$5 \times 10^2$	$1.1 \times 10^{-3}$	$8.7 \times 10^{-4}$	$8.6 \times 10^{-3}$	—	—	—
$10^3$	$7.7 \times 10^{-3}$	$5.1 \times 10^{-3}$	$5.7 \times 10^{-2}$	—	—	—
$5 \times 10^3$	$1.7 \times 10^{-1}$	$1.9 \times 10^{-1}$	$4.7 \times 10^{-1}$	$6.6 \times 10^{-4}$	$2.2 \times 10^{-3}$	$6.9 \times 10^{-4}$
$10^4$	$4.9 \times 10^{-1}$	$6.6 \times 10^{-1}$	1.0	$1.7 \times 10^{-2}$	$4.5 \times 10^{-2}$	$1.7 \times 10^{-2}$
$5 \times 10^4$	4.4	6.0	5.0	1.1	2.1	1.1

seen in Table III(b).

We compare the present results with those of Midorikawa and Yoshimura.<sup>6)</sup> They mainly studied the cross-sections due to the mechanism II. The present results are found to be about 2 times larger than theirs, which came from the

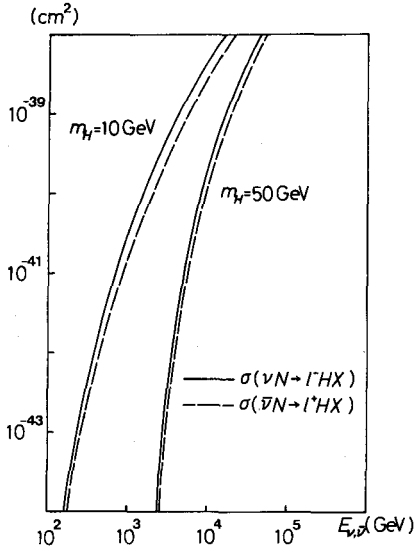


Fig. 3(a)

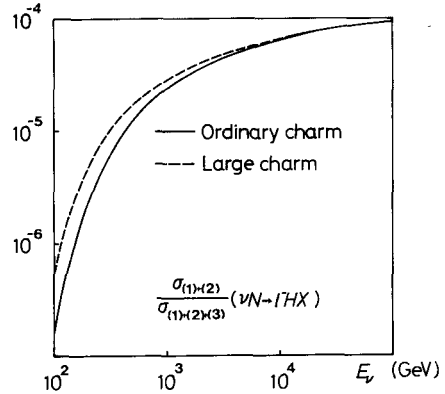


Fig. 3(b)

Fig. 3(a) Energy dependence of the total cross-sections  $\sigma(\nu N \rightarrow l^- HX)$  (solid lines) and  $\sigma(\bar{\nu} N \rightarrow l^+ HX)$  (dashed lines) in Lab-frame. Two left lines are for the case  $m_H = 10$  GeV and others are for  $m_H = 50$  GeV.

(b) Comparison of the contributions of the bremsstrahlung from heavy quark (strange- and charm-quark) and weak boson ( $W^\pm$  or  $Z$  boson) in  $\nu N \rightarrow l^- HX$  process for the case  $m_H = 10$  GeV (in Lab-frame).  $\sigma_{(1)+(2)}$  and  $\sigma_{(1)+(2)+(3)}$  denote the cross-sections calculated by using the diagrams (1)+(2) and (1)+(2)+(3) in Fig. 2.1 respectively. "Ordinary charm" (solid line) corresponds to the charm distribution function by Buras and Gaemers and "Large charm" (dashed line) corresponds to the assumed distribution Eq. (3.1).

(c) Lab-energy dependence of the total cross-section  $\sigma(l^- N \rightarrow l^- HX)$ . The left (dashed) line, the middle (solid) line and the right (solid) line represent the case i)  $m_H = 10$  GeV and the large intrinsic charm, ii)  $m_H = 10$  GeV and the ordinary charm, and iii)  $m_H = 50$  GeV and the ordinary charm respectively.

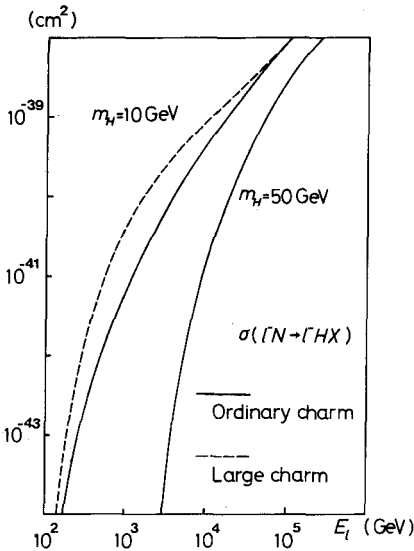


Fig. 3(c)

rough numerical computations in Ref. 6).\*) (Using the formulas given by them, we have re-calculated the cross-sections, and obtained consistent results with the present ones.) They also computed the cross-sections due to the mechanism I within the approximation of soft Higgs boson emission. As is expected from the nature of this approximation, their results are larger than ours.

Finally, in addition to these comparisons, it should be mentioned that there still remain rather inevitable ambiguities in the results (though they are small in comparison with the discrepancies mentioned above) concerning the form of parton distribution, although we have made calculations exactly. That is, the total cross-sections are sensitive to the parton distribution function, especially, in low energy region due to the existence of the threshold. As an example, we compare the results (in  $10^{-39} \text{ cm}^2$  unit) obtained by using the distribution parametrized by Barger et al. (solution 2 in Ref. 11)) with the present ones (case (2) in Table III(a)) for  $\sigma(\nu_l N \rightarrow l^- H X)$ :

$E_\nu(\text{GeV})$	Buras-Gaemers (without QCD effects)	Barger et al.
$10^2$	$2.8 \times 10^{-7}$	$9.6 \times 10^{-8}$
$5 \times 10^4$	$6.2 \times 10$	$5.0 \times 10$

We should keep in mind these uncertainties.

#### § 4. Discussion

We have made calculations of lepton-induced Higgs boson productions for extensive range of laboratory energy. The main results are summarized as follows.

i)  $\nu N$  process: The bremsstrahlung from  $W^\pm$  boson (mechanism II) gives dominant contribution, and that from heavy quarks (mechanism I) is negligible even at very high energy where the heavy quark contents in the nucleon are considerably enhanced by the QCD effects. Therefore it seems to be totally difficult to test the possibility of large intrinsic charm model.

ii)  $l^- N$  process: In this process, the bremsstrahlung from heavy quark occurs via photon exchange, i. e., the "electromagnetic interaction" while the process by the mechanism II is the "weak" process. This difference causes the situation that the former mechanism gives almost the same contribution as that of the latter mechanism. Consequently, the increase of the charm component in the nucleon (large intrinsic charm model) produces the visible effect in the total cross-section as shown in Fig. 3(c).

\*) In Ref. 6), numerical integrations were performed by the Gauss method. As is well-known, Monte Carlo method is more reliable than the Gauss method for multiple integrals.

iii) The results are sensitive to the form of parton distribution functions, especially in low energy region due to the threshold.

In the following we consider experimental feasibilities to catch the Higgs production effect. One possibility seems to look at the relation to the neutrino induced same-sign dimuon event the origin of which is still unclear.\*) The Higgs boson production can induce  $\mu^-\mu^-$  pair as follows :

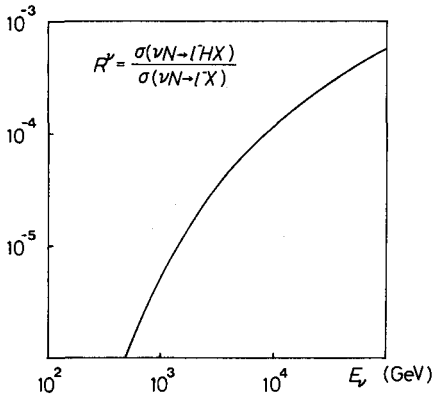
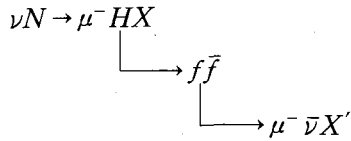


Fig. 4(a) Lab-energy dependence of the ratio  $R^\nu \equiv \sigma(\nu N \rightarrow l^- HX) / \sigma(\nu N \rightarrow l^- X)$  for the case  $m_H = 10$  GeV.

( $f$  denotes a heavy fermion with  $2m_f < m_H$ ).

Unfortunately, however, we have obtained a negative conclusion from the comparison between  $\sigma(\nu N \rightarrow l^- HX)$  and  $\sigma(\nu N \rightarrow l^- X)$ . We show the ratio  $R^\nu \equiv \sigma(\nu N \rightarrow l^- HX) / \sigma(\nu N \rightarrow l^- X)$  for the case  $m_H = 10$  GeV in Fig. 4(a). The ratio is found to be too small to explain the experimental data  $\sigma(\nu N \rightarrow \mu^-\mu^- X) / \sigma(\nu N \rightarrow \mu^- X) \sim 10^{-3}$  at  $E_\nu \lesssim 100$  GeV.

As another possibility, let us consider the experiment of high energy  $ep$  collider. We take the following values<sup>13)</sup> for energies and  $L$ (luminosity) as a representative experimental setup :

$$E_e = 20 \text{ GeV} \quad \text{and} \quad E_p = 300 \text{ GeV},$$

$$(s \simeq 2.4 \times 10^4 \text{ GeV}^2)$$

$$L = 4.6 \times 10^{31} \text{ cm}^{-2} \text{ sec}^{-1}.$$

These conditions lead to the expected event rate :

$$\sigma^{ep} \cdot L \simeq 3.0 \times 10^{-8} \text{ sec}^{-1}, \quad (\text{for } m_H = 10 \text{ GeV}) \quad (4.1)$$

that is, 1 event per about 380 days. In the case of the large intrinsic charm model, the result changes to 1 event per 200 days. If we can get the same luminosity at,

\* ) Concerning the present situation on this event (including experimental data), see Ref. 12).

e. g., 10 times higher energy ( $s \approx 2.4 \times 10^5$ ), the result is 17~18 events/year (for both ordinary and large charm cases). Anyway high energy and large luminosity are necessary to catch the Higgs boson in lepton-nucleon scatterings.

The above discussions are restricted to the case of  $m_H = 10$  GeV and four quark flavors. There seems to be possibilities of enhancement of the total cross-sections in other cases, e.g., extremely light Higgs boson and/or  $b$  quark excitation in the nucleon. The contribution of  $b$  quark is estimated to be  $(3/2)^2$  times larger than that of charm-quark ( $m_b/m_c \approx 3$  and  $|Q_b|/|Q_c| = 1/2$ ) in high energy region where  $c(x, Q^2)$  and  $b(x, Q^2)$  give the same contribution. Actually, however, this  $b$  quark contribution will not enhance the total cross-sections drastically since the contribution of the diagram (3) will dominate at such very high energy (as is expected from the case of the neutrino reaction). On the other hand, the possibility of extremely light Higgs boson is not favored by some theoretical consideration.<sup>3)</sup> Therefore we do not consider these possibilities here any more.

Let us give a conclusion. The lepton-induced Higgs boson productions are interesting processes from the theoretical point of view since, for example, we can see QCD effects clearly through the production from heavy quark (Fig. 3(b)). Experimentally, however, we must conclude that lepton-nucleon processes are not good places for the detection of the Higgs boson unless an accelerator with energy and luminosity much higher than those presently available or planned in the near future is constructed.

### Acknowledgements

We would like to thank Professor S. Matsuda, Dr. M. Bando, Professor H. Terazawa, Professor T. Shimada and all the participants of the seminars at Research Institute for Fundamental Physics, Department of Physics, Kyoto University, and Department of Physics, Osaka University for stimulative discussions. We also thank Professor S. Matsuda for careful reading of the manuscript, and Dr. A. Bodec for suggestive communication without which this work would not have been done. One of us (Z.H.) is grateful to Professor M. Morita for warm hospitality at Department of Physics, Osaka University. We (Z. H., S. M. and H. N.) respectively acknowledge the Osaka Univ. Yukawa foundation, the Yukawa foundation and the Japan society for the promotion of science for financial supports.

### References

- 1) S. L. Glashow, Nucl. Phys. **22** (1961) 579.  
S. Weinberg, Phys. Rev. Letters **19** (1967), 1264.  
A. Salam, *Elementary Particle Theory: Relativistic Groups and Analyticity* (Nobel

- Symposium No. 8) ed. by N. Svartholm (Almqvist and Wiksell, Stockholm, 1968), p. 367.  
S. L. Glashow, J. Iliopoulos and L. Maiani, Phys. Rev. **D2** (1970), 1285.  
M. Kobayashi and T. Maskawa, Prog. Theor. Phys. **49** (1973), 652.
- 2) For example, K-I. Aoki, Z. Hioki, R. Kawabe, M. Konuma and T. Muta, Prog. Theor. Phys. Suppl. No. 73 (1982).
  - 3) A. D. Linde, JETP Letters **23** (1976) 64.  
S. Weinberg, Phys. Rev. Letters **36** (1976), 294.
  - 4) B. W. Lee, C. Quigg and H. B. Thacker, Phys. Rev. **D16** (1977), 1519.  
N. Cabibbo, L. Maiani, G. Parisi and R. Petronzio, Nucl. Phys. **B158** (1979), 295.  
H. Komatsu, Prog. Theor. Phys. **65** (1981), 779.
  - 5) J. Ellis, M. K. Gaillard and D. V. Nanopoulos, Nucl. Phys. **B106** (1976), 292.  
J. M. LoSecco, Phys. Rev. **D14** (1976), 1352.  
R. M. Godbole, Phys. Rev. **D18** (1978), 95.  
K. O. Mikaelian and R. J. Oakes, *Proceedings of the 1978 DUMAND Summer Workshop* (1978), p. 89.
  - 6) S. Midorikawa and M. Yoshimura, Nucl. Phys. **B162** (1980), 365.
  - 7) J. Abad, J. L. Alonso, A. Cruz, M. Fontannaz, D. Schiff and B. Pire, Phys. Rev. **D24** (1981), 2837.
  - 8) S. J. Brodsky, C. Peterson and N. Sakai, Phys. Rev. **D23** (1981), 2745.
  - 9) A. J. Buras and K. J. F. Gaemers, Nucl. Phys. **B132** (1978), 249.
  - 10) G. P. Lepage, Cornell Preprint, CLNS-80/447 (1980).
  - 11) V. Barger, T. Weiler and R. J. N. Phillips, Nucl. Phys. **B102** (1976), 439.
  - 12) V. Barger, W. Y. Keung and R. J. N. Phillips, Phys. Rev. **D25** (1982), 1803.
  - 13) *Report of the TRISTAN ep (e $\bar{e}$ ) Working Group* (UTPN-165 and UT-345), ed. by T. Kamae, Y. Shimizu and M. Igarashi (1980), Chap. 2.